Some issues concerning large-eddy simulation of inertial particle dispersion in turbulent bounded flows

C. Marchioli,[1] M. V. Salvetti,[2] and A. Soldati[1,a)]

[1]*Department of Energy Technology and Centro Interdipartimentale di Fluidodinamica e Idraulica,*
University of Udine, 33100 Udine, Italy
[2]*Department of Aerospace Engineering, University of Pisa, 56100 Pisa, Italy*

The problem of accurate Eulerian–Lagrangian modeling of inertial particle dispersion in large-eddy simulation (LES) of turbulent wall-bounded flows is addressed. We run direct numerical simulation (DNS) of turbulent channel flow at shear Reynolds number $Re_\tau = 150$ and corresponding *a priori* and *a posteriori* LES on two coarser grids. For each flow field, we tracked swarms of particles with different inertia to examine the behavior of particle statistics, specifically focusing on particle preferential segregation and accumulation at the wall. Our object is to discuss the necessity of a closure model for the particle equations when using LES and we verify if the influence of the subgrid turbulence filtered by LES is an important effect on particle motion according to particle size. The results show that well-resolved LES gives particle velocity statistics in satisfactory agreement with DNS. However, independent of the grid, quantitatively inaccurate predictions are obtained for local particle preferential segregation, particularly in the near-wall region. Inaccuracies are observed for the entire range of particle size considered in this study, even when the particle response time is much larger than the flow time scales not resolved in LES. The satisfactory behavior of LES in reproducing particle velocity statistics is thus counterbalanced by the inaccurate representation of local segregation phenomena, indicating that closure models supplying the particle motion equation with an adequate rendering of the flow field might be needed. Finally, we remark that recovering the level of fluid and particle velocity fluctuations in the particle equations does not ensure a quantitative *replica* of the subgrid turbulence effects, thus implying that accurate subgrid closure models for particles may require information also proportional to the higher-order moments of the velocity fluctuations. © *2008 American Institute of Physics*.
[DOI: 10.1063/1.2911018]

I. INTRODUCTION

The dispersion of inertial particles in turbulent flows is characterized by macroscopic phenomena such as nonhomogeneous distribution, large-scale clustering, and preferential concentration due to the inertial bias between the denser particles and the lighter surrounding fluid.[1,2] In homogeneous isotropic turbulence,[1,3,4] clustering and preferential concentration may be crucial in determining collision frequency, breakage efficiency, agglomeration, and reaction rates. In turbulent boundary layers, besides controlling particle interaction rates, clustering and preferential concentration also influence settling, deposition and entrainment.[5]

Both direct numerical simulation[6] (DNS) and large-eddy simulation[7–9] (LES) together with Lagrangian particle tracking (LPT) have been used to investigate and quantify the behavior of particles near the wall, for instance, in channel flow[2,8,9] or in pipe flow.[6,7] DNS-based Eulerian–Lagrangian studies are used to investigate the physics of particle-turbulence interactions, whereas LES has yet to demonstrate its full capabilities in predicting correctly particle-turbulence statistics[10] and macroscopic segregation phenomena.[4,9] To

elaborate, in LES-based Eulerian–Lagrangian simulations of particle dispersion, a *subgrid* error is introduced in the particle equation since only the filtered fluid velocity is available; this approximation adds to the *modeling* error which is intrinsic to the subgrid scale (SGS) modeling for the fluid phase.[10] Similar to what is done for the flow field, a way to model the effects of the SGS velocity fluctuations in the particle equations of motion could be identified for those situations in which subgrid and modeling errors affect the predicting capabilities of LES.[9]

Among previous LES applications to gas-solid turbulent flows,[7,11] the fluid SGS velocity fluctuations were neglected under the assumption that the particle response time was large compared to the smallest time scale resolved in the LES.[11] For well-resolved LES, this assumption holds to capture satisfactorily the statistics of particle velocity.[7,10,11] However, it was later demonstrated that LES without any SGS model for particles gives a certain degree of inaccuracy in the prediction of particle accumulation at the wall. We refer, in particular, to the results obtained by Kuerten and Vreman[10] and by Kuerten[9] for turbulent dispersion of heavy particles in channel flow. They have shown that, due to both subgrid and modeling errors, LES underestimates the tendency of particles to move toward the wall by the effect of turbulence (turbophoretic effect[12]). To circumvent this prob-

---

     20, 040603-1

lem, a closure model for the particle equation of motion based on filter inversion by approximate deconvolution was proposed to recover the influence of the filtered scales. Searching for further effects of the filtered scales, Fede and Simonin[4] have investigated homogeneous isotropic turbulence. They have shown that, limiting to single particle statistics such as turbulent dispersion, this influence is negligible when the particle response time is much larger than the cutoff time scale of the subgrid velocities. However, they also show that accumulation and collision phenomena are strongly influenced by subgrid fluid turbulence even when the particle response time is up to $\mathcal{O}(10)$ times the Kolmogorov time scale.

In this work, we want to address some issues which are still open in bounded flows, where local particle segregation is a crucial phenomenon controlling particle wall deposition and re-entrainment.[2,13] Considering as benchmark a DNS of turbulent channel flow at shear Reynolds number $\mathrm{Re}_\tau = 150$ in which we tracked swarms of inertial particles, we run accurate *a priori* and *a posteriori* LES to examine the behavior of particle velocity statistics. In our view, this analysis, done for different LES grid resolutions and for different particle sizes, may indicate the upper limits of LES in reproducing correctly such statistics, possibly confirming and extending to grid sensitivity the work of Kuerten and Vreman.[10] In addition, we want to more deeply explore the reasons of LES inaccuracy in predicting particle deposition. We believe[2,5] that these reasons are associated with local particle segregation in the buffer region of the turbulent boundary layer. This may be useful to ascertain if closure models capable of introducing the fluctuating energy back into the filtered flow field are sufficiently accurate or, rather, if some further information on the flow structure at the subgrid level is required.

This paper is organized as follows. Problem statement, governing equations and numerical methodology required for the simulations are presented in Sec. II. Section III is devoted to the analysis and discussion of relevant statistics obtained from simulations where particle trajectories are computed from DNS, filtered DNS in a *a priori* tests and LES in *a posteriori* tests. The discussion will be focused on the quantification of subgrid and modeling errors on particle velocity and concentration statistics as well as on particle preferential distribution. Finally, conclusions and future developments are drawn in Sec. IV.

II. PHYSICAL PROBLEM AND NUMERICAL METHODOLOGY

A. Particle-laden turbulent channel flow

The flow into which particles are introduced is a turbulent channel flow of gas. In the present study, we consider air (assumed to be incompressible and Newtonian) with density $\rho = 1.3$ kg m^{-3} and kinematic viscosity $\nu = 15.7 \times 10^{-6}$ m^2 s^{-1}. The governing balance equations for the fluid (in dimensionless form) read as

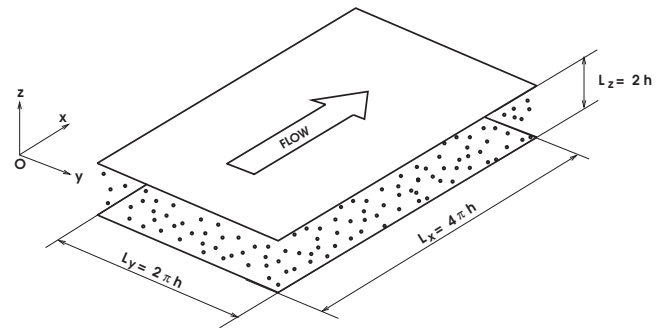$$\frac{\partial u_i}{\partial x_i} = 0, \qquad (1)$$

FIG. 1. Particle-laden turbulent gas flow in a flat channel: computational domain.

$$\frac{\partial u_i}{\partial t} = -u_j \frac{\partial u_i}{\partial x_j} + \frac{1}{\mathrm{Re}} \frac{\partial^2 u_i}{\partial x_j^2} - \frac{\partial p}{\partial x_i} + \delta_{1,i}, \qquad (2)$$

where u_i is the ith component of the dimensionless velocity vector, p is the fluctuating kinematic pressure, $\delta_{1,i}$ is the mean dimensionless pressure gradient that drives the flow and $\mathrm{Re}_\tau = u_\tau h / \nu$ is the shear Reynolds number based on the shear (or friction) velocity, u_τ, and on the half channel height, h. The shear velocity is defined as $u_\tau = (\tau_w / \rho)^{1/2}$, where τ_w is the mean shear stress at the wall. All variables considered in this study are reported in dimensionless form, represented by the superscript $+$ (which has been dropped from Eqs. (1) and (2) for easier reading) and expressed in wall units. Wall units are obtained by combining u_τ, ν, and ρ.

In LES, the standard continuity and Navier–Stokes equations are smoothed with a filter function of width Δ. Accordingly, all flow variables are decomposed into a resolved (large-scale) part and a residual (subgrid scale) part as $\mathbf{u}(\mathbf{x}, t) = \bar{\mathbf{u}}(\mathbf{x}, t) + \delta \mathbf{u}(\mathbf{x}, t)$. The filtered continuity and Navier–Stokes equations for the resolved scales are then

$$\frac{\partial \bar{u}_i}{\partial x_j} = 0, \qquad (3)$$

$$\frac{\partial \bar{u}_i}{\partial t} = -\bar{u}_j \frac{\partial \bar{u}_i}{\partial x_j} + \frac{1}{\mathrm{Re}} \frac{\partial^2 \bar{u}_i}{\partial x_j^2} - \frac{\partial \bar{p}}{\partial x_i} + \delta_{1,i} - \frac{\partial \tau_{ij}}{\partial x_j}, \qquad (4)$$

where $\tau_{ij} = \overline{u_i u_j} - \bar{u}_i \bar{u}_j$ represents the SGS stress tensor. The large-eddy dynamics is closed once a model for τ_{ij} is provided. In the present study, the dynamic SGS model of Germano *et al.*[14] has been applied.

The reference geometry consists of two infinite flat parallel walls: the origin of the coordinate system is located at the center of the channel and the $x-$, $y-$, and $z-$ axes point in the streamwise, spanwise, and wall-normal directions, respectively (see Fig. 1). Periodic boundary conditions are imposed on the fluid velocity field in x and y, and no-slip boundary conditions are imposed at the walls. The calculations were performed on a computational domain of size $4\pi h \times 2\pi h \times 2\ h$ in x, y, and z, respectively.

Particles with density $\rho_p = 1000$ kg m^{-3} are injected into the flow at concentration low enough to consider dilute system conditions. The motion of particles is described by a set of ordinary differential equations for particle velocity and

position. For particles much heavier than the fluid ($\rho_p / \rho \gg 1$), Elghobashi and Truesdell[15] have shown that the most significant forces are the Stokes drag and buoyancy and that Basset force can be neglected being one order of magnitude smaller. In the present simulations, the aim is to minimize the number of degrees of freedom by keeping the simulation setting as simplified as possible; thus the effect of gravity has also been neglected. With the above assumptions, a simplified version of the Basset–Boussinesq–Oseen equation[16] is obtained. In vector form

$$\frac{d\mathbf{x}}{dt} = \mathbf{v}, \tag{5}$$

$$\frac{d\mathbf{v}}{dt} = -\frac{3}{4}\frac{C_D}{d_p}\left(\frac{\rho}{\rho_p}\right)|\mathbf{v} - \mathbf{u}|(\mathbf{v} - \mathbf{u}), \tag{6}$$

where $\mathbf{x}$ is the particle position, $\mathbf{v}$ is the particle velocity, and $\mathbf{u}$ is the fluid velocity at particle position. The Stokes drag coefficient is computed as $C_D = 24/\mathrm{Re}_p(1 + 0.15\mathrm{Re}_p^{0.687})$, where $\mathrm{Re}_p = d_p|\mathbf{v} - \mathbf{u}|/\nu$ is the particle Reynolds number and d_p is the particle diameter. The correction for C_D is necessary when Re_p does not remain small.

B. DNS and LES methodology

In this study, DNS and LES have been applied to fully developed channel flow. In both cases, the governing equations are discretized using a pseudospectral method based on transforming the field variables into wave number space, using Fourier representations for the periodic streamwise and spanwise directions and a Chebyshev representation for the wall-normal (nonhomogeneous) direction. A two-level, explicit Adams–Bashforth scheme for the nonlinear terms, and an implicit Crank–Nicolson method for the viscous terms are employed for time advancement. Further details of the method have been published previously.[17]

TABLE I. Summary of the simulations.

Re$_\tau$	DNS	*a priori* LES	*a posteriori* LES
150	$128 \times 128 \times 129$	$64 \times 64 \times 129$ (CF=2)	$64 \times 64 \times 65$
		$32 \times 32 \times 129$ (CF=4)	$32 \times 32 \times 65$
		$16 \times 16 \times 129$ (CF=8)	$\cdots$

DNS calculations have been performed at shear Reynolds number $\mathrm{Re}_\tau = 150$ ($u_\tau = 0.117\,75$ m s^{-1}). The corresponding bulk Reynolds number is $\mathrm{Re}_b = u_b h/\nu = 2100$, where $u_b \simeq 1.65$ m s^{-1} is the bulk (average) velocity. The size of the computational domain in wall units is $1885 \times 942 \times 300$, discretized in physical space with $128 \times 128 \times 129$ grid points (corresponding to 128×128 Fourier modes and to 129 Chebyshev coefficients in the wave number space). This is the minimum number of grid points required in each direction to ensure that the grid spacing is always smaller than the smallest flow scale and that the limitations imposed by the point-particle approach are satisfied.[18]

LES calculations have been performed using the serial version of the pseudospectral flow solver on the same computational domain. Two computational grids have been considered: a *coarse* grid made of $32 \times 32 \times 65$ nodes and a *fine* grid made of $64 \times 64 \times 65$ nodes.

The complete set of DNS/LES simulations is summarized in Table I.

C. Filtering for *a priori* tests

In the *a priori* tests, LPT is carried out starting from the filtered velocity field, $\bar{\mathbf{u}}$, obtained through explicit filtering of the DNS velocity by means of either a cutoff filter or a top-hat filter. Both filters are applied in the homogeneous streamwise and spanwise directions in the wave number space:

$$\bar{u}_i(\mathbf{x},t) = \mathrm{FT}^{-1}\begin{cases} G(\kappa_1)G(\kappa_2)\hat{u}_i(\kappa_1,\kappa_2,z,t) & \text{if } |\kappa_j| \leq |\kappa_c| \quad \text{with } j=1,2, \\ 0 & \text{otherwise}. \end{cases} \tag{7}$$

where FT is the 2D Fourier transform, $\kappa_c = \pi/\Delta$ is the cutoff wave number (Δ being the filter width in the physical space), $\hat{u}_i(\kappa_1,\kappa_2,z,t)$ is the Fourier transform of the fluid velocity field, namely, $\hat{u}_i(\kappa_1,\kappa_2,z,t) = \mathrm{FT}[u_i(\mathbf{x},t)]$ and $G(\kappa_j)$ is the filter transfer function:

$$G(\kappa_j) = \begin{cases} 1 & \text{for the cutoff filter}, \\ \dfrac{\sin(\kappa_j\Delta/2)}{\kappa_j\Delta/2} & \text{for the top-hat filter}. \end{cases} \tag{8}$$

Three different filter widths have been considered, corresponding to a grid coarsening factor (CF in Table I) in each

homogeneous direction of 2, 4, and 8 with respect to DNS. In the wall-normal direction, data are not filtered, since often in LES the wall-normal resolution is DNS-like.[19]

D. Lagrangian particle tracking

To calculate particle trajectories in the flow field, we have coupled a Lagrangian tracking routine with the DNS/LES flow solver. The routine solves for Eqs. (6) and (5) using sixth-order Lagrangian polynomials to interpolate fluid velocities at particle position; with this velocity the equations of particle motion are advanced in time using a fourth-order Runge–Kutta scheme. The time step size used for particle

TABLE II. Particle parameters for the simulations.

St	τ_p (s)	d_p^+	d_p (μm)	$V_s^+ = g^+$St	$Re_p^+ = V_s^+ d_p^+ / \nu^+$
0.2	0.227×10^{-3}	0.068	9.1	0.0188	0.001 28
1	1.133×10^{-3}	0.153	20.4	0.0943	0.014 43
5	5.660×10^{-3}	0.342	45.6	0.4717	0.161 32
25	28.32×10^{-3}	0.765	102.0	2.3584	1.804 18
125	1.415×10^{-1}	1.71	228	11.792	20.16 43

tracking was chosen to be equal to the time step size used for the fluid, $\delta t^+ = 0.045$; the total tracking time was, for each particle set, $\Delta t^+ = 1200$ in the *a priori* tests and $\Delta t^+ = 1800$ in the *a posteriori* tests. These simulation times are not long enough to achieve a statistically steady state for the particle concentration.[20] Elaborating, we have $T_l < \Delta t^+ < T_L$, where $T_l \simeq$ St represents the time scale taken by the particle to reach a condition of local equilibrium with the surrounding fluid and T_L represents the time scale required to reach a statistically steady particle concentration (in the present simulations, the estimated value of T_L for the intermediate size particles is equal to 180 times the through-flow period, defined as the time for fluid particles in the middle of the channel to sweep the domain along the streamwise direction). We will present averaged statistics which do not depend on the time behavior of particle distribution like the particle root mean square (rms) velocity components. These quantities scale with T_l and simulation times comparable to Δt^+ are sufficient to compute steady-state values. We will also present instantaneous particle concentration statistics and particle segregation statistics, which scale with T_L and will be in transient state. From an engineering viewpoint, we are interested in this physical situation because it is the most probable for a dispersed flow. In a number of industrial applications, including separation[21] and droplet-laden flows,[22] particle distribution never reaches equilibrium.

Particles, which are assumed pointwise, rigid, and spherical, are injected into the flow at concentration low enough to neglect particle collisions. The effect of particles onto the turbulent field is also neglected (one-way coupling assumption). At the beginning of the simulation, particles are distributed homogeneously over the computational domain and their initial velocity is set equal to that of the fluid at the particle initial position. Periodic boundary conditions are imposed on particles moving outside the computational domain in the homogeneous directions, perfectly elastic collisions at the smooth walls are assumed when the particle center is at a distance lower than one particle radius from the wall.

For the simulations presented here, large samples of 10^5 particles, characterized by different response times, were considered. The particle response time is defined as $\tau_p = \rho_p d_p^2 / 18 \mu$, where μ is the fluid dynamic viscosity: when the particle response time is made dimensionless using wall variables, the Stokes number for each particle set is obtained as St $= \tau_p^+ = \tau_p / \tau_f$ where $\tau_f = \nu / u_\tau^2$ is the viscous time scale of the flow. Table II shows all the parameters of the particles injected into the flow field. We remark here that, for the present channel flow configuration, the nondimensional

value of the Kolmogorov time scale, τ_K^+, ranges from 2 wall units at the wall to 13 wall units at the channel centerline.[23] Hence, if we rescale the particle response times given in Table II using the local value of τ_K^+ near the centerline, where the flow conditions are closer to homogeneous and isotropic, we obtain Stokes numbers that vary from 10^{-2} to 10 and fall in the lower range of values considered by Fede and Simonin.[4]

III. RESULTS

A. Particle distribution in *a priori* LES

In this section, we will discuss the influence of filtering on particle distribution by showing the velocity statistics and the concentration profiles for particles dispersed in *a priori* LES flow fields, i.e., filtered DNS fields corresponding to ideal LES fields with no modeling error for the fluid. We will also discuss filtering effects on local particle preferential segregation using a macroscopic segregation parameter. As described in Sec. II C, the cutoff and the top-hat filters have been used. The cutoff filter provides a sharp separation between resolved and nonresolved scales and can be considered the filter corresponding to a coarse spectral simulation, in which no explicit filtering is applied. Conversely, the top-hat filter is a smooth filter and, therefore, it subtracts a significant amount of energy from the resolved scales.[24] For each filter, three different filter widths have been considered. Figure 2 sketches the effect of these filter widths on the one-dimensional (streamwise) frequency spectrum, $E(\omega)$.[25] Since particle dynamics in the viscous sublayer is controlled by flow structures with nondimensional time scale $\tau_f^+ \simeq 25$ and considering that this time scale corresponds to the circulation time of the turbulence structures in the buffer layer ($5 < z^+ < 30$),[13] we show the energy spectrum at the $z^+ = 25$ location. The cutoff frequencies corresponding to each filter width are indicated as $\omega_{\text{cutoff}}^{\text{CF}=2}$, $\omega_{\text{cutoff}}^{\text{CF}=4}$, and $\omega_{\text{cutoff}}^{\text{CF}=8}$ in increasing order. Also shown (dot-dashed lines) are the estimated response frequencies which characterize each particle set considered in the *a priori* tests, these frequencies being proportional to $1/\tau_p$. Areas filled with patterns below the energy profile represent the relative amount of energy removed by each filter width: larger filter widths prevent particles from being exposed to ever-increasing turbulent frequencies, namely, to smaller and smaller flow scales which can modify significantly their local behavior, dispersion, and segregation. Inaccurate estimation of these processes due to filtering will bring subgrid errors into subsequent particle motion.

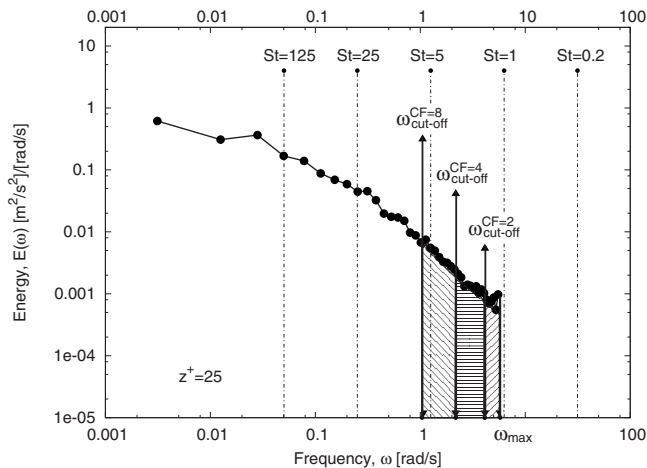Figure 3 shows the particle rms velocity fluctuations ob-

FIG. 2. One-dimensional (streamwise) frequency spectrum for turbulent channel flow computed at $z^+=25$. The different cutoff frequencies, used to perform the *a priori* tests, are indicated as $\omega_{cutoff}^{CF=2}$, $\omega_{cutoff}^{CF=4}$, and $\omega_{cutoff}^{CF=8}$, respectively. Areas filled with patterns below the energy profile represent the relative amount of energy removed by each cutoff.

tained in the *a priori* tests with cutoff filter for the St=1, the St=5, and the St=25 particles, respectively. The reference values obtained injecting the particles in the DNS flow field are also reported. Specifically, the streamwise and wall-normal rms components are shown in Figs. 3(a)–3(c) and in Figs. 3(d)–3(f). All profiles were obtained averaging in time (from $t^+=450$ to $t^+=1200$) and space (over the homogeneous directions). Filtering the fluid velocity can have a large impact on the behavior of the turbulent velocity fluctuations. Particle velocity fluctuations at a CF=2 filter width (corresponding to a well-resolved ideal LES in which the SGS modeling error for the fluid is negligible) are nearly the same as those obtained in DNS: limiting to these statistics, LES

ensures a reasonably accurate description of the flow field. Quantitative discrepancies become more evident for the larger filter widths (coarse LES), because particle fluctuations are reduced. This is a consequence of the well-known decrease of the flow velocity fluctuations due to filtering as felt by the particles, even if in a different measure depending on their inertia. Note, however, that the effect of filtering is also significant on particles having characteristic response frequencies much lower than those removed by the filters (e.g., the St=25 particles).

For the cutoff filter, underestimation of the particle fluctuations is a pure effect of the elimination of the SGS scales, since no energy is subtracted from the resolved ones. The results obtained with the top-hat filter (not shown here for brevity) are qualitatively similar, although, for a given filter width, underestimation of the particle fluctuations is, as expected, larger than that obtained using the cutoff filter.

The reduction of the wall-normal velocity fluctuations near the wall for the *a priori* LES, shown in Figs. 3(d)–3(f), is worth noting because, particularly in the limit of small Stokes number, it corresponds to a reduction of particle turbophoretic drift (namely, particle migration to the wall in turbulent boundary layers) and, in turn, to a reduction of particle accumulation in the near-wall region.[10] This is also shown in Fig. 4, where the near-wall instantaneous particle concentration obtained at time $t^+=1200$ in *a priori* LES is compared to the DNS one for different filter widths and different particle inertia. It appears that the tendency of particles to cluster near the wall is qualitatively captured in the *a priori* tests. Yet, filtering leads to an underestimation of the wall particle concentration, for all filter types and widths and for all particle sets considered in this study. Note that this is observed also when the cutoff filter of smallest width is used [Figs. 4(a)–4(c) and 4(e)], for which the level of fluctuations
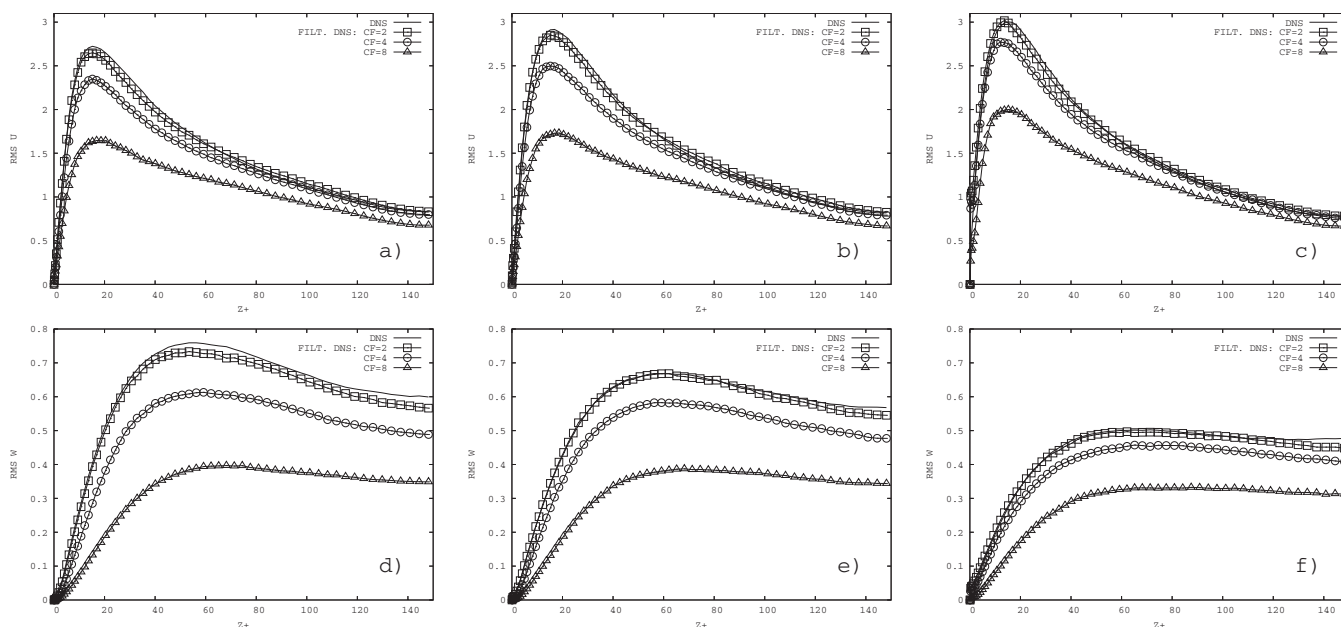

FIG. 3. Particle rms velocity fluctuations for *a priori* simulations (with cutoff filter) without SGS modeling in the particle equation of motion: [(a)–(c)] streamwise rms component, [(d)–(f)] wall-normal rms component. Left-hand panels: St=1 particles, central panels: St=5 particles, right-hand panels: St=25 particles. CF indicates the LES grid coarsening factor with respect to the DNS grid: CF=2 (□), CF=4 (○), and CF=8 (△).
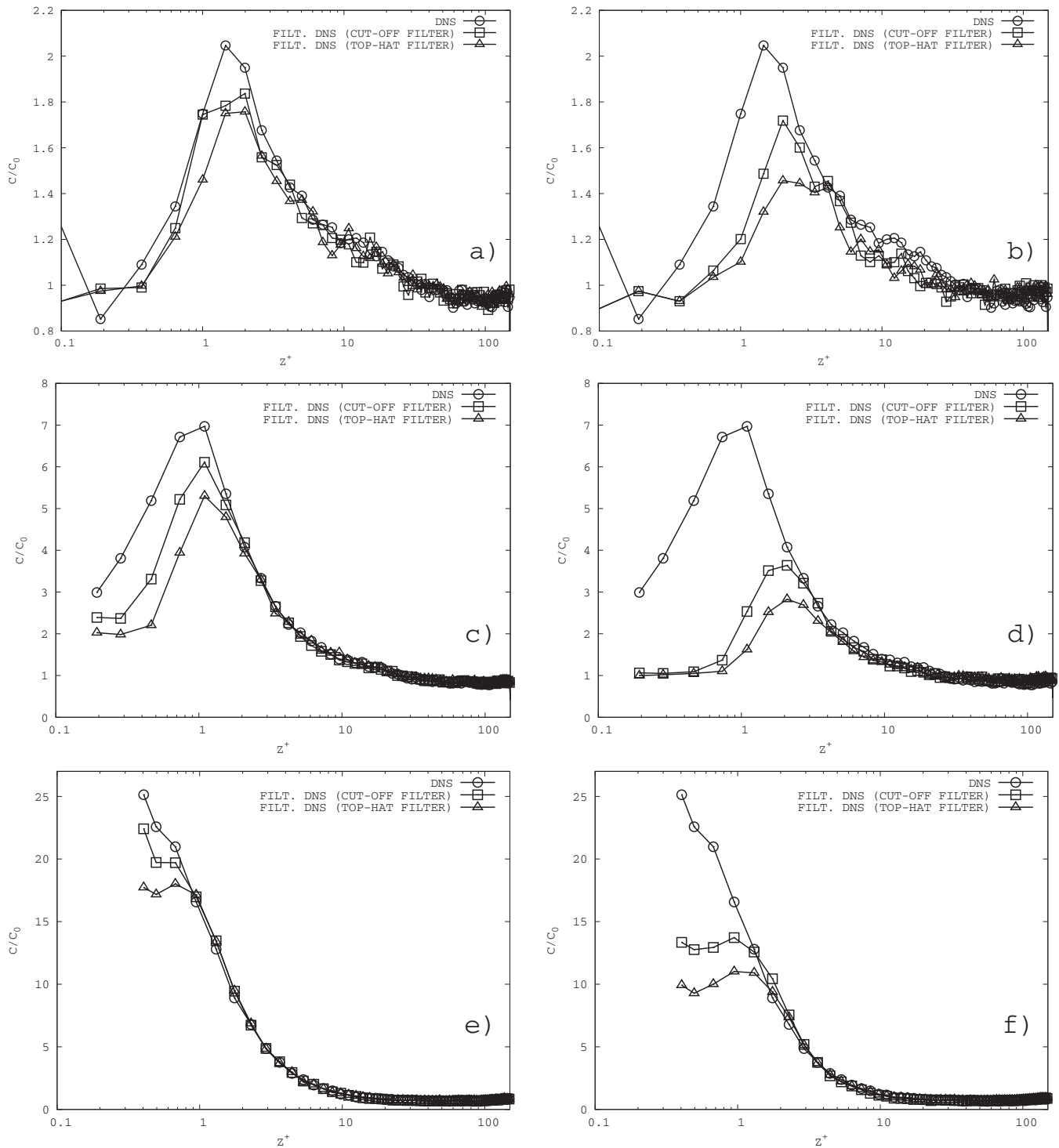
FIG. 4. Particle concentration in *a priori* tests without SGS modeling in the particle equation of motion: [(a) and (b)] St=1 particles, [(c) and (d)] St=5 particles, [(e) and (f)] St=25 particles. DNS (○), *a priori* LES with cutoff filter (□), *a priori* LES with top-hat filter (△). Left-hand panels: tests on the fine $64 \times 64 \times 65$ grid (CF=2); right-hand panels: tests on the coarse $32 \times 32 \times 65$ grid (CF=4).

of both fluid and particle velocities is very close to the DNS one. In this case, however, deviations from the DNS reference value are mainly limited to a few percent with peaks in the range of 10%–15% very close to the wall (within one wall unit). Percentages increase significantly for the larger filter [Figs. 4(b)–4(d)].[10] We remark that these estimates are relative to statistically developing particle concentration and, therefore, the concentration values will change at later simu-

lation times. However, upon also examining many different time instants, we observe that the tendency is always the same as that shown in Fig. 4.

To explore further the need of a SGS closure model for particles, in Fig. 5, we plot the particle segregation parameter, Σ_p, as a function of the particle Stokes number in two different regions of the channel: the channel centerline, where Σ_p has been computed in a fluid slab 10 wall unit
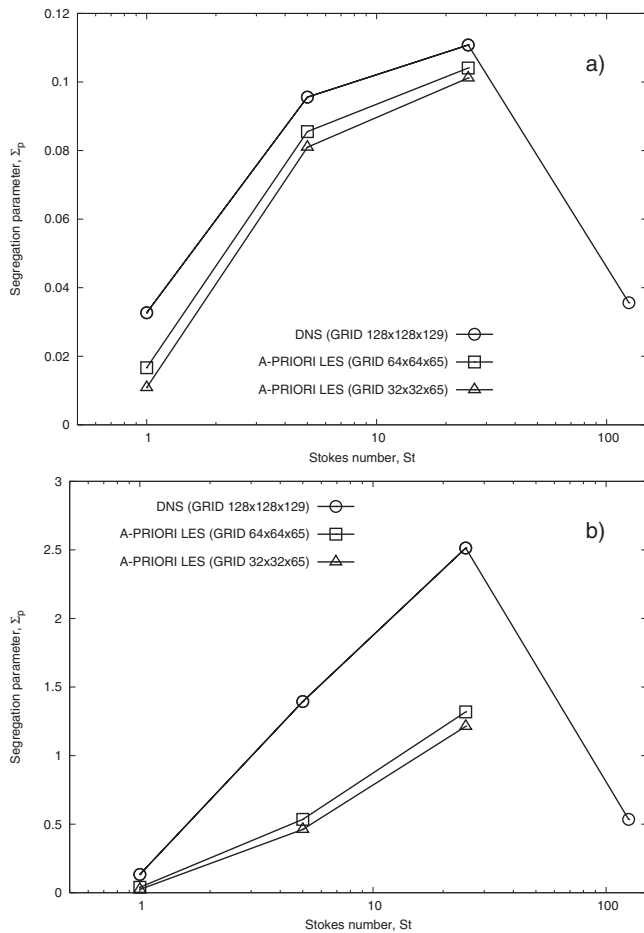
FIG. 5. Particle segregation, Σ_p, vs particle Stokes number St in turbulent channel flow: comparison between DNS ($\bigcirc$), *a priori* LES on the fine $64 \times 64 \times 65$ grid ($\square$) and *a priori* LES on the coarse $32 \times 32 \times 65$ grid ($\triangle$). *A priori* results are relative to the cutoff filter. Panels: (a) channel centerline ($145 \leqslant z^+ \leqslant 150$), (b) near-wall region ($0 \leqslant z^+ \leqslant 5$).
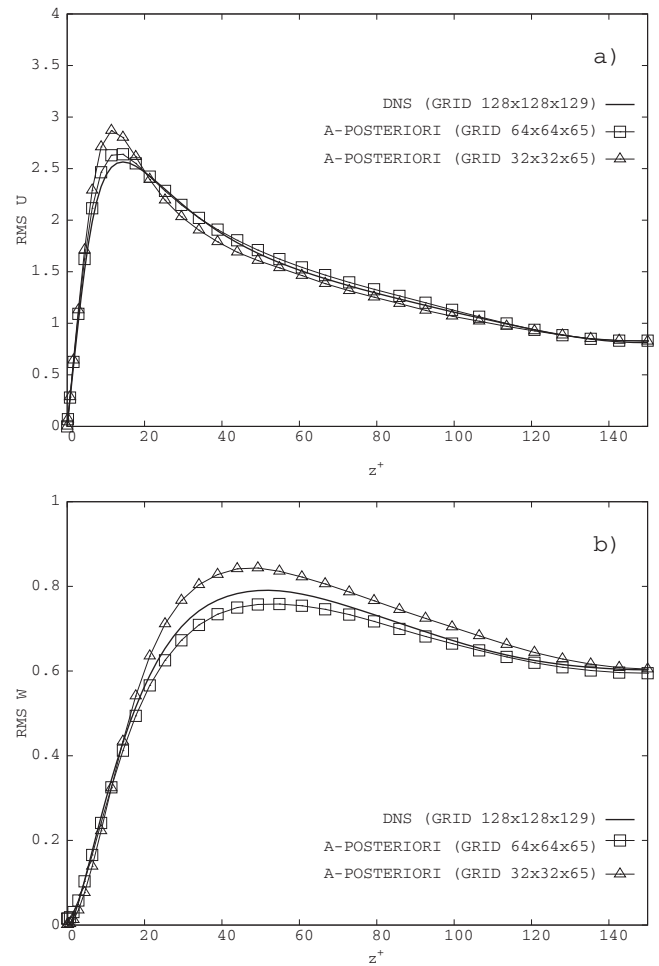

FIG. 6. Fluid rms velocity fluctuations: comparison between DNS (solid line), *a posteriori* LES on the fine $64 \times 64 \times 65$ grid ($\square$) and *a posteriori* LES on the coarse $32 \times 32 \times 65$ grid ($\triangle$). Panels: (a) streamwise rms component and (b) wall-normal rms component.

thick centered at $z^+ = 150$, and in the near-wall region, where Σ_p has been computed in the viscous sublayer ($0 \leqslant z^+ \leqslant 5$). The segregation parameter (or maximum deviation from randomness)[26] is used here to compare the relative tendency of particles to segregate in a turbulent flow field. As evident from previous results, LES can provide a reliable representation of some features of the flow field, such as velocity statistics and energy (this being true even from a quantitative viewpoint when LES is well resolved). However, the issue we try to address here is whether these "modeled" features are enough to adequately reproduce the statistics of particle dispersion. Following previous studies (see Rouson and Eaton,[26] or Février *et al.*[27] among others), we use Σ_p to answer this question.

The segregation parameter is calculated as $(\sigma - \sigma_{\text{Poisson}})/m$, where σ and σ_{Poisson} represent the standard deviations for the particle number density distribution and the Poisson distribution, respectively. The particle number density distribution is computed on a grid containing N_{cell} cells of volume Ω_{cell} covering the entire computational domain. This grid is, for all simulations (including DNS), independent of the Eulerian grid used by the flow solvers. The parameter m is the mean number of particles in one cell for a

random uniform particle distribution.[26,28] The drawback of this method is the dependence of Σ_p on the cell size. To avoid this problem, we computed the particle number density distribution for several values of Ω_{cell} and we kept only the largest value of Σ_p.[27] We remark here that Ω_{cell} is varied by changing the streamwise and the spanwise lengths of the cell whereas the wall-normal length is maintained to a uniform thickness (equal for LES and DNS) to avoid the introduction of an additional averaging scale in the direction perpendicular to the wall. Interestingly, our calculations show that the largest Σ_p is obtained for the same cell volume both in DNS and in LES, for a given Stokes number. Also, for a given cell volume, the values of Σ_p for particles dispersed in the LES flow field are always smaller than those for particles dispersed in the DNS flow field.

As found in previous studies,[13] at $\text{Re}_\tau = 150$, a peak of Σ_p occurs for $\text{St} \simeq 25$ and preferential concentration falls off on either side of this *optimum* value. The St=25 particles are thus the most responsive to the near-wall turbulent structures. When an explicit filter is applied, particle segregation is underpredicted in all considered cases, especially near the wall. Note that this underestimation is significant also for the smallest filter width, for which the reduction of particle fluc-
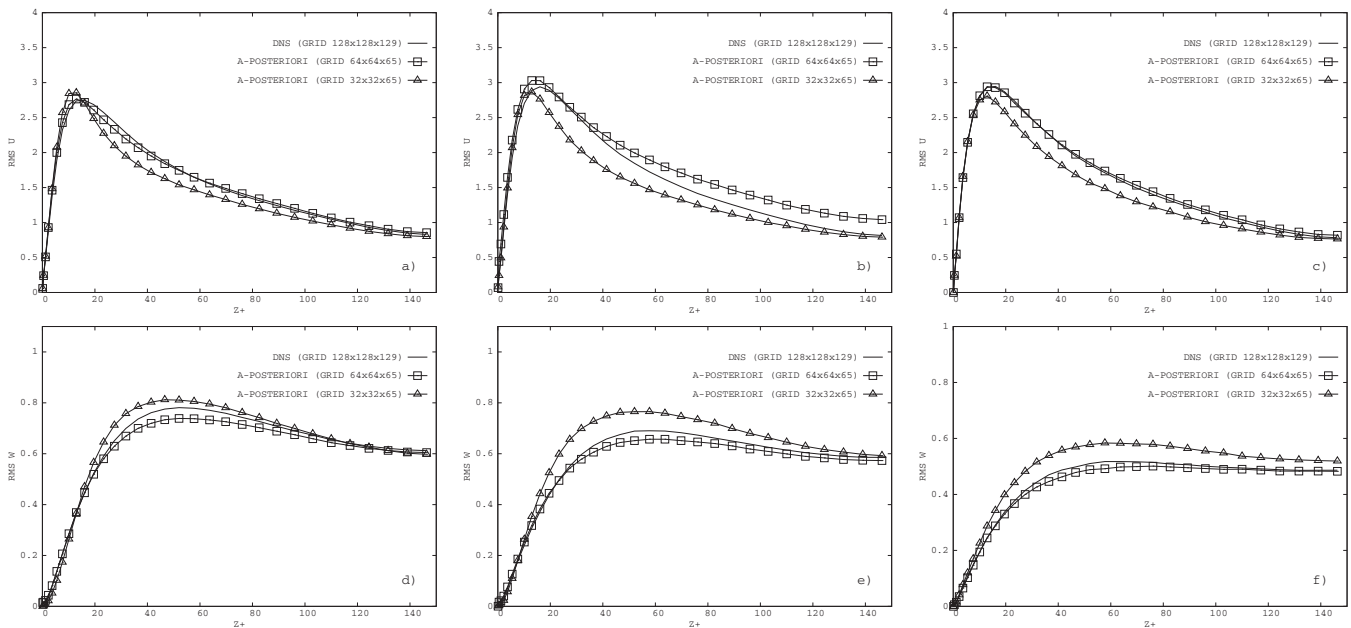
FIG. 7. Particle rms velocity fluctuations: comparison between DNS (solid line), *a posteriori* LES on the fine $64 \times 64 \times 65$ grid ($\square$) and *a posteriori* LES on the coarse $32 \times 32 \times 65$ grid ($\triangle$): (a)–(c) streamwise rms component, (d)–(f) wall-normal rms component. Left-hand panels: St=1 particles, central panels: St=5 particles, right-hand panels: St=25 particles.

tuations was relatively small (see Fig. 3). From a physical viewpoint, these results seem to indicate that particles segregate less in LES fields. Particle deposition is the outcome of a three-stage process; first, the dispersed phase is segregated into clusters localized around the large vortical structures of the flow; second, clusters are transported by the instantaneous realizations of the fluid Reynolds stresses toward the wall, where deposition occurs; finally, once at the wall particles/droplets remain trapped by turbulent vortical structures in the viscous sublayer, where particle concentration eventually increases. According to this scenario, we hypothesize that weaker deposition fluxes and, in turn, lower near-wall accumulation correspond to segregation underestimated by LES.

B. Particle distribution in *a posteriori* LES

In this section, we will discuss the behavior of particles dispersed in *a posteriori* LES flow fields. Two different LES grids have been used, as shown in Table I. In these tests, different sources of errors are present in addition to the filtering effects discussed in Sec. III A, viz., the errors due to (i) the SGS modeling for the fluid phase, (ii) the numerical discretization of the fluid governing equations, and (iii) the interpolation in the Lagrangian particle tracking. For the used pseudospectral discretization the numerical error should plausibly be negligible. As for interpolation, a sixth-order interpolation scheme is used. Although we did not carry out a sensitivity study, the analysis in Kuerten and Vreman[10] indicates that the interpolation error should remain small, even if it may introduce an additional smoothing. Thus, we believe that the main source of difference with the *a priori* tests is represented by the SGS model closing the governing equations for the fluid phase. As in the *a priori* tests, no closure model is used in the equations of particle motion.

In order to asses the quality of the LES for the fluid part, Fig. 6 compares the streamwise and wall-normal rms of the fluid velocity components obtained in LES to the reference DNS values. For the LES on the fine grid, a good agreement with DNS is obtained and, hence, this can be considered as a well-resolved LES for the fluid phase. Conversely, in the coarser LES, significant errors are found in the prediction of the fluid phase velocity fluctuations and, thus, errors in the Lagrangian particle tracking are anticipated. The effect of the SGS modeling error is clearly visible if the values obtained for the coarser grid are compared to those of the *a priori* tests (see Fig. 3) for a corresponding coarsening factor (CF=4). Indeed, in the *a posteriori* LES, the introduction of the SGS model for the fluid equations tends to counteract the decrease of the fluid velocity fluctuations due to filtering; in the coarser case, this leads to an overestimation of the rms of the streamwise and wall-normal velocity components. This overestimation is a rather well-known behavior of coarse LES, especially for the rms of the streamwise component. Nonetheless, it is worth remarking that in actual LES the fluid velocity fields in which the particles are dispersed are not always characterized by a lack of fluctuations, as it happens in the idealized context of *a priori* tests.

We do not show here results which were obtained with the Smagorinsky SGS model. These simulations led to statistics generally less accurate than those obtained with the dynamic eddy-viscosity model for a fixed grid resolution.[14]

In Fig. 7, the streamwise and wall-normal rms of the different particle sets obtained in LES are compared to the reference DNS data. A good agreement with DNS is obtained in the well-resolved LES for all the considered particle inertia, while significant discrepancies are found in the coarser simulation. Note that in the coarse LES, the rms of the wall-normal velocity component are overestimated for all the con-

sidered particle sets, as previously observed also for the fluid phase. This overestimation should anticipate higher net wall-ward particle fluxes and, in turn, concentration peaks higher than the DNS ones. In spite of this, the underestimation of particle concentration at the wall, already observed in the *a priori* tests (see Sec. III A), is also found in the *a posteriori* LES for all considered resolutions and for all particle sets. This is shown, for instance, by the instantaneous particle concentration profiles of Fig. 8, where quantitative deviations with respect to the DNS reference value can become quite large. Consider, for instance, the small St=1 particles: deviations are in the range of 5–10% with a peak of roughly 50% near the wall for the well-resolved LES, and they grow up to 10–15% with a peak of roughly 100% near the wall for the coarse LES. For the intermediate St=5 particles, deviations are even larger. For these two particle sets, the expected effect due to the rms overshoot is not visible because it is overcompensated by an opposite effect due to a lack of accuracy in reproducing the fine-scale features of the turbulent field. Following Kuerten and Vreman,[10] the LES may produce an inaccurate rendering of the near-wall vortices responsible for trapping particles in the viscous sublayer. When these vortices are smeared out, the microscale interaction between near-wall turbulence structures and particles cannot be fully captured, particle trapping is underestimated and the net wallward fluxes of particles decrease. This latter effect is less important for the St=25 particles, whose concentration profile in the coarse LES is actually closer to the DNS one compared to the well-resolved LES. These particles have high inertia and, thus, their deposition is less influenced by the fine turbulence structures in the near-wall region. The effect of the SGS fluid velocities on these particles is also smaller, and the increase of accumulation due to the rms overshoot prevails (note that, consistently, there is no rms overshoot in the well-resolved LES).

The solution provided by the flow solver (be it DNS or LES) coupled with the particle solver (LPT, in our case) within one viscous wall unit or fractions might be slightly affected by limitations in the modeling, yet these limitations should have a negligible effect when performing a comparative analysis. In this respect, we believe that the differences in the concentration statistics discussed above do indicate that LES is able to capture particle near-wall accumulation from a qualitative viewpoint, yet not from a purely quantitative viewpoint (particularly in the near-wall region). The same observation holds also for particle segregation, which is rather well estimated in the channel centerline [Fig. 2(a)], but severely underestimated in the viscous sublayer [Fig. 2(b)]. We can thus remark that errors in the quantitative prediction of both particle segregation and near-wall accumulation occur even if fluid and particle velocity fluctuations are well predicted, suggesting that reintroducing the correct level of velocity fluctuations in the particle equations is not the only issue to design an accurate closure model.

Finally, in the *a posteriori* LES the segregation parameter, Σ_p, was also computed for St=125 particles (see Fig. 9). For this set of particles, the values obtained in both large-eddy simulations are higher than those computed in DNS. In their *a priori* tests for homogeneous and isotropic turbulence,
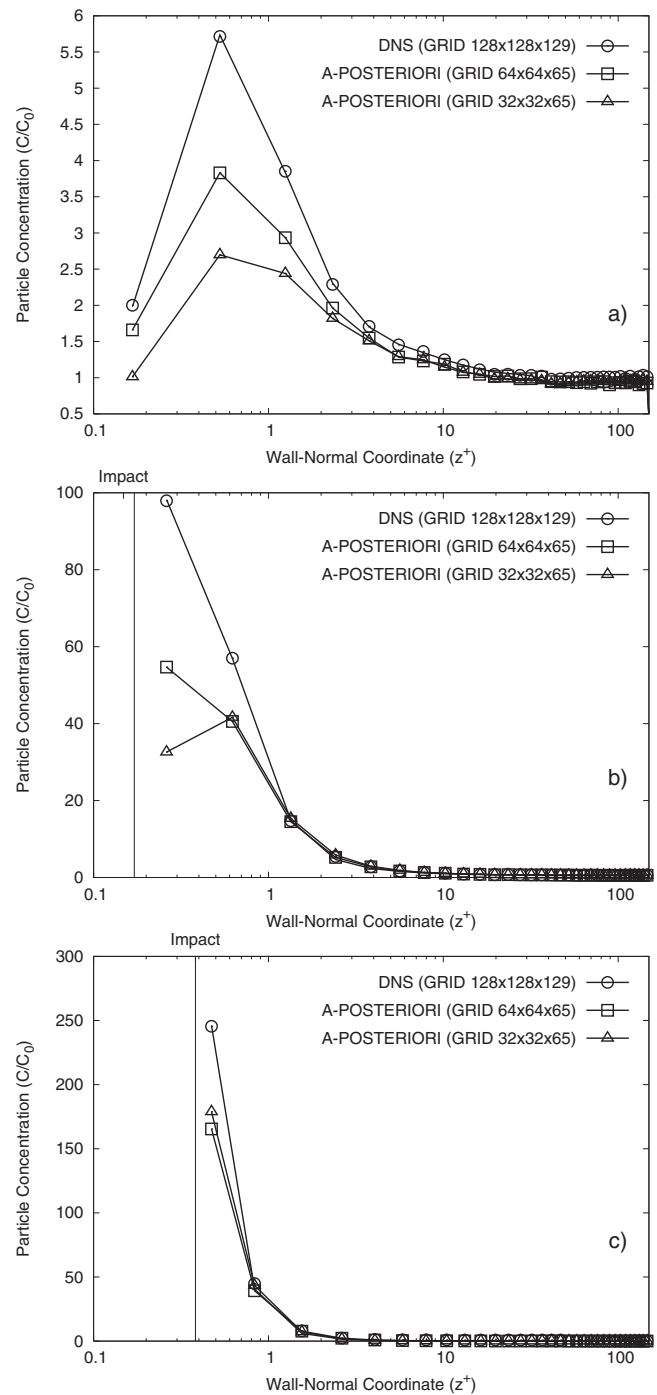

FIG. 8. Particle concentration in *a posteriori* tests without SGS modeling in the particle equation of motion: comparison between DNS ($\bigcirc$), *a posteriori* LES on the fine $64 \times 64 \times 65$ grid ($\square$) and *a posteriori* LES on the coarse $32 \times 32 \times 65$ grid ($\triangle$). Panels: (a) St=1 particles, (b) St=5 particles, and (c) St=25 particles. The vertical solid line in each diagram indicates the position where the particles hit the wall (impact): note that impact for the St =1 particles occurs at $z^+=0.034$, outside the z^+ range covered in panel (a).

Fede and Simonin[4] found that for particles having lower inertia than a given threshold value, the effect of filtering was to decrease the segregation parameter, while for particles of larger inertia the segregation was conversely increased. From our results, this scenario seems to hold also in *a posteriori* LES and in near-wall turbulence.
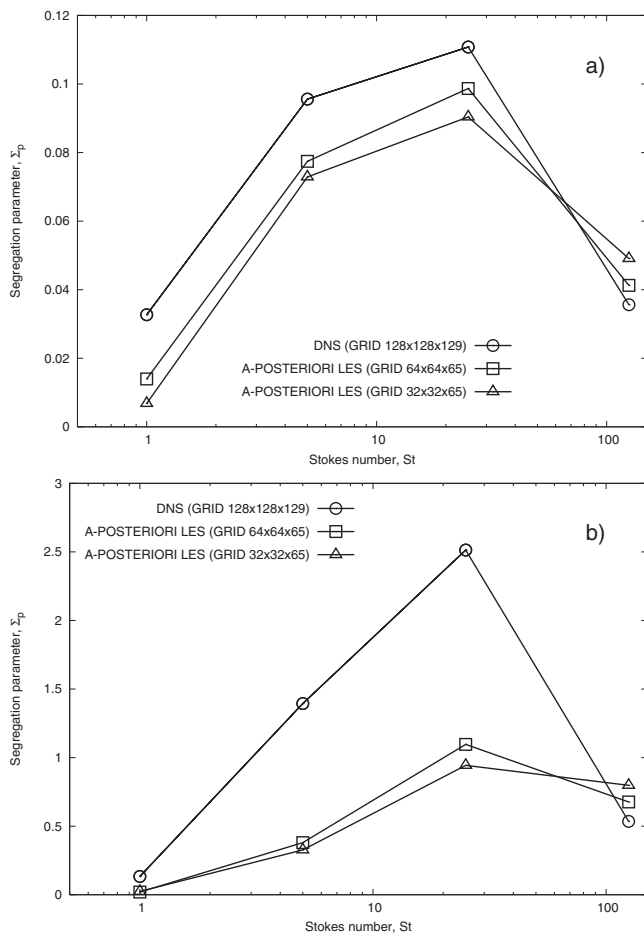
FIG. 9. Particle segregation, Σ_p, vs particle Stokes number, St, in turbulent channel flow: comparison between DNS ($\bigcirc$), *a posteriori* LES on the fine $64 \times 64 \times 65$ grid ($\square$) and *a posteriori* LES on the coarse $32 \times 32 \times 65$ grid ($\triangle$). Panels: (a) channel centerline ($145 \leqslant z^+ \leqslant 150$) and (b) near-wall region ($0 \leqslant z^+ \leqslant 5$).

IV. CONCLUSIONS AND FUTURE DEVELOPMENTS

In this paper, we address some open issues relative to the modeling of heavy particle dispersion in large–eddy simulation. Considering as benchmark a DNS of turbulent channel flow at shear Reynolds number $Re_\tau = 150$ in which we tracked swarms of inertial particles, we run accurate *a priori* and *a posteriori* LES to examine the influence of the subgrid turbulence filtered by LES on particle statistics, focusing our attention on local particle segregation and on particle accumulation at the wall. Our objectives are to investigate the influence of filtering on particle segregation and accumulation and to discuss the necessity of using closure models for the equations of particle motion to improve the prediction of these phenomena when using LES. The analysis is performed in a systematic way for different particle inertia (obtained by tuning of the particle size with respect to the filtered spatial scales) and for different resolutions of the LES grid. The accuracy in the prediction of the particle velocity statistics is assessed through *vis-à-vis* comparison against DNS data.

The effect of pure filtering in *a priori* simulations is to decrease the fluid velocity fluctuations and, in turn, the particle velocity fluctuations, although by different amounts ac-

cording to particle inertia. Our simulations demonstrate that particle accumulation at the wall is underestimated by the different LES for the entire range of particle response times considered in this study. These findings confirm the results of Kuerten and Vreman[10] and extend their conclusions also to different LES grid resolutions.

Wall deposition of particles, namely, particle wall flux, controls wall concentration and is a by-product of local particle segregation in specific areas of the buffer region.[5] We thus examined particle preferential concentration performing in-depth analysis of the behavior of the segregation parameter. Results show that filtering leads to a significant underestimation of this parameter. Surprisingly, inaccuracies were observed also when the amount of the filtered fluid velocity fluctuations is small, namely, for the cutoff filter at the finest resolution.

In *a posteriori* simulations, when a fine grid (two times the DNS grid spacing in each direction) and the dynamic SGS model are used, a correct level of fluid velocity fluctuations is obtained; the particle velocity fluctuations are also in good agreement with those obtained in DNS. Conversely, significant discrepancies are observed with respect to the DNS reference values when a coarser resolution (typical of LES grids) is used. The velocity fluctuations of both phases are overestimated, in contrast with the *a priori* tests. In spite of these differences, particle wall accumulation and local segregation are always underestimated.

These results just summarized seem to indicate that, from a qualitative viewpoint, LES can reproduce some features of a turbulent flow field (velocity statistics, for instance), and yet it may be judged inaccurate as far as the quantitative prediction of local particle segregation and accumulation (particularly in the near-wall region) is concerned. In this case, a closure model supplying the particle equations with a satisfactory representation of the flow field might improve the quantitative agreement between LES and DNS.[8–10,29] The degree of improvement granted by such model is an important issue that needs to be clarified. In particular, it must be ascertained if recovering the correct level of fluid and particle velocity fluctuations can warrant accurate prediction of near-wall accumulation and local particle segregation. Considering our results, we feel that some additional information on the flow structures at the subgrid level is required. This piece of information could perhaps be retrieved using non-Gaussian stochastic Lagrangian models based on Langevin-type equations[30] to reintroduce the correct amount of higher-order moments of the velocity fluctuations in the particle equations.

[1] L. P. Wang and M. R. Maxey, "Settling velocity and concentration distribution of heavy particles in homogeneous isotropic turbulence," J. Fluid Mech. **256**, 27 (1993).

[2] C. Marchioli and A. Soldati, "Mechanisms for particle transfer and segregation in turbulent boundary layer," J. Fluid Mech. **468**, 283 (2002).

[3] J. Bec, L. Biferale, M. Cencini, A. Lanotte, S. Musacchio, and F. Toschi, "Heavy particle concentration in turbulence at dissipative and inertial scales," Phys. Rev. Lett. **98**, 084502 (2007).

[4] P. Fede and O. Simonin, "Numerical study of the subgrid fluid turbulence effects on the statistics of heavy colliding particles," Phys. Fluids **18**, 045103 (2006).

[5] A. Soldati, "Particles turbulence interactions in boundary layers," Z. Angew. Math. Mech. **85**, 683 (2005).

[6] C. Marchioli, A. Giusti, M. V. Salvetti, and A. Soldati, "Direct numerical simulation of particle wall transfer and deposition in upward turbulent pipe flow," Int. J. Multiphase Flow **29**, 1017 (2003).

[7] W. S. J. Uijttewaal and R. W. A. Oliemans, "Particle dispersion and deposition in direct numerical and large eddy simulations of vertical pipe flows," Phys. Fluids **8**, 2590 (1996).

[8] Q. Wang and K. D. Squires, "Large eddy simulation of particle deposition in a vertical turbulent channel flow," Int. J. Multiphase Flow **22**, 667 (1996).

[9] J. G. M. Kuerten, "Subgrid modeling in particle-laden channel flow," Phys. Fluids **18**, 025108 (2006).

[10] J. G. M. Kuerten and A. W. Vreman, "Can turbophoresis be predicted by large-eddy simulation?," Phys. Fluids **17**, 011701 (2005).

[11] V. Armenio, U. Piomelli, and V. Fiorotto, "Effect of the subgrid scales on particle motion," Phys. Fluids **11**, 3030 (1999).

[12] M. W. Reeks, "The transport of discrete particles in inhomogeneous turbulence," J. Aerosol Sci. **14**, 729 (1983).

[13] M. Picciotto, C. Marchioli, and A. Soldati, "Characterization of near-wall accumulation regions for inertial particles in turbulent boundary layers," Phys. Fluids **17**, 098101 (2005).

[14] M. Germano, U. Piomelli, P. Moin, and W. H. Cabot, "A dynamic subgrid-scale eddy viscosity model," Phys. Fluids **3**, 1760 (1991).

[15] S. E. Elghobashi and G. C. Truesdell, "Direct simulation of particle dispersion in a decaying isotropic turbulence," J. Fluid Mech. **242**, 655 (1992).

[16] C. Crowe, M. Sommerfeld, and T. Tsuji, *Multiphase Flows With Droplets and Particles* (CRC, New York, 1998).

[17] Y. Pan and S. Banerjee, "Numerical simulation of particle interactions with wall turbulence," Phys. Fluids **8**, 2733 (1996).

[18] In the present flow configuration, the nondimensional Kolmogorov length scale, η_K^+, varies along the wall-normal direction from a minimum value $\eta_K^+=1.6$ at the wall to a maximum value $\eta_K^+=3.6$ at the centerline. The grid resolution in the wall-normal direction is such that the first collocation point is at $z^+=0.05$ from the wall, while in the center of the channel $\Delta z^+=3.7$.

[19] S. Pope, "Ten questions concerning the large-eddy simulation of turbulent flows," New J. Phys. **6**, 1 (2004).

[20] C. Marchioli, A. Soldati, J. G. M. Kuerten, B. Arcen, A. Tanière, G. Goldensoph, K. D. Squires, M. F. Cargnelutti, and L. M. Portela, "Statistics of particle dispersion in direct numerical simulations of wall-bounded turbulence: Results of an international collaborative benchmark test," Int. J. Multiphase Flow (to be published).

[21] A. Soldati, "On the influence of electrohydrodynamics and turbulence on particle transport and collection efficiency in wire-plate electrostatic precipitators," J. Aerosol Sci. **31**, 293 (2000).

[22] A. Soldati and P. Andreussi, "The influence of coalescence on droplet transfer in vertical annular flow," Chem. Eng. Sci. **51**, 353 (1996).

[23] C. Marchioli, M. Picciotto, and A. Soldati, "Particle dispersion and wall-dependent fluid scales in turbulent bounded flow: Implications for local equilibrium models," J. Turbul. **27**, 1 (2006).

[24] P. Sagaut, *Large Eddy Simulation for incompressible flows* (Springer-Verlag, Berlin, 2001).

[25] S. Pope, *Turbulent flows* (Cambridge University Press, Cambridge 2000).

[26] D. W. Rouson and J. K. Eaton, "On the preferential concentration of solid particles in turbulent channel flow," J. Fluid Mech. **428**, 149 (2001).

[27] P. Février, O. Simonin, and K. D. Squires, "Partitioning of particle velocities in gas-solid turbulent flows into a continuous field and a spatially-uncorrelated random distribution: Theoretical formalism and numerical study," J. Fluid Mech. **533**, 1 (2005).

[28] Here, random is defined as the situation in which any given particle is equally likely to appear in any given cell so that one can show that the particle number distribution approaches a Poisson distribution [see Rouson and Eaton (Ref. 26)].

[29] B. Shotorban and F. Mashayek, "Modeling subgrid-scale effetcs on particles by approximate deconvolution," Phys. Fluids **17**, 081701 (2005).

[30] I. Iliopoulos and T. J. Hanratty, "A non-Gaussian stochastic model to describe passive tracer dispersion and its comparison to a direct numerical simulation," Phys. Fluids **16**, 3006 (2004).